Preparation of Nonlethal Projectiles by Polyurethane Foam with the Dynamic and Microscopic Characterization for Risk Assessment and Management

Noureddine Boumdouha,* Zitouni Safidine, and Achraf Boudiaf

Read Online

ACCESS | Metrics & More | Article Recommendations | SI Supporting Information

ABSTRACT: Nonlethal projectiles are manufactured and designed proportionately, with a minimal likelihood of mortality or harm. However, numerous real-world examples indicate that nonlethal projectiles can potentially inflict severe lesions and death in some circumstances. As a result, it is essential to design and manage the manufacture of projectile materials to achieve maximum efficacy with the least amount of collateral damage. The current paper provides a technique for generating and analyzing filled polyurethane (PU) foams and studying their viscoelastic characteristics. The sand and graphite composition ranged between 5 and 10% by weight. The suggested technique seeks to exert control over the evolution of the microstructure. The mechanical characteristics were obtained by dynamic mechanical analysis (DMA) testing. We made a pneumatic launcher and a sturdy rigid wall. In addition, the artificial human head is covered with force sensors to perform dynamic characterization. Also, scanning electron microscopy (SEM) of the polyurethane foam cross sections demonstrated that the average cell size of 98 μm was unaffected by the fillings' content. Furthermore, X-ray diffraction analysis (XRD) characterized the developmental foams' physicochemical properties. Finally, we assessed the dynamic search for nonlethal projectiles. We recorded the viscous criteria (VC$_{max}$) values to check for nonlethal projectiles.
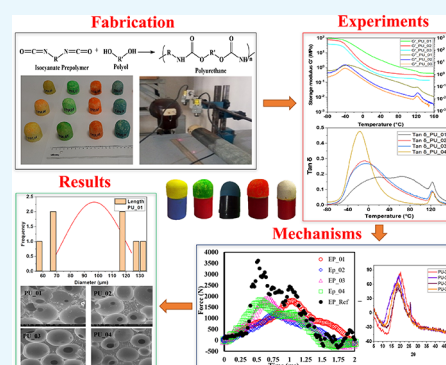
1. INTRODUCTION

Nonlethal kinetic energy uses weapons to transfer sufficient influence to a person to deter their dangerous and illegal behavior without causing permanent harm to them. For example, nonlethal projectiles are used to neutralize and incapacitate people in riots, crowd control, and the interception of suspicious marine craft. They offer an alternative to an adequate response by guaranteeing neutralization without causing permanent injuries to the targeted targets. There is a wide range of products on the market. Nevertheless, the study focuses on the characterization of different degrees of polyurethane foams.[1,2]

There are several reported cases of serious injuries or even death following the use of this type of projectile. Therefore, it is essential to associate the manufacturing process with the assessment of the lesion risk of these projectiles to avoid any situation that would be contrary to the doctrine of the use of nonlethal projectile weapons. Various materials are used to ensure the soft use of nonlethal projectile weapons, in which modified polyurethane foam is generally used.[3] In this age of community-based police, the use of the most morally appropriate and ethical ways of maintaining harmony, law, and order is evident. The least ethically and compassionately acceptable sort of hurt would be less lethal. However, when struggling with criminals and cop casualties, the usefulness of the less-lethal gun device from the officer's viewpoint is another big problem. Unfortunately, most research has not studied different forms of small, deadly firearms suitable for law enforcement.

The primary difficulty with nonlethal weapon choices is a general lack of study into their performance. Studies evaluating the efficacy of nonlethal arms devices are produced most frequently by commodity producers. The law enforcement authorities are then forced to focus on factory details, specification sheets, and business ads to decide the essential implementation framework. The producers can exploit this knowledge conveniently for themselves. This article aims at reviewing, as a guide, the existing literature on using force frames for the following sections, which discuss a variety of nonlethal weapons.[4]

Research scientists have not yet studied the efficacy of less destructive gun structures at the official level, where force is used, meetings usually occur, although there is substantial

scientific literature on the use of police. According to existing literature studies, most scholars focused on discriminatory brutality, unnecessary force, and exploitation of fatalities. It dramatically demonstrates the difference between death and a less fatal force that can assert power over an individual but not destroy or harm him.[5] They deal with the light-based, nonlethal force of what is deemed socially permissible. More debate is included about the possible unintentional effects of force assault.

This study addresses some of the main challenges around the police and security services doctrine in the state's respect for civil rights and democracy.[6] Of course, these nonlethal projectiles need the push of a single button to perform their mission. Still, the policeman's responsibility is much greater in undermining the rule of law without bias. Filming police officers in action has never been easier, which means misconduct is more likely to be caught than before.[7] And just like us, every time a video comes out showing an officer abusing his power, many people say, "Well, I would have done this differently."

The use of force by the police has tremendous repercussions for officers of the law department and the government. Thus, the use of force may also affect foreign policy formulation and implementation. Present public legislation authorizes officers to employ the least volume of power required to influence arrests or curb disorder, using equipment at their discretion (e.g., toxic weapons, armaments of effect, defensive tactics). Unfortunately, there is no less dangerous weapon that suits these situations. While such options, such as nonlethal projectiles, tend to provide total rewards for suspected enforcement and a decrease in both offenders' and officers' accidents,[8] their portfolio is limited. Moreover, to allow the use of the nonlethal projectile, officials would then position themselves inside a 21-foot criminal radius, posing additional threats and logistical considerations.

On the other hand, weapons (e.g., less deadly bullets such as nonlethal projectiles) react reasonably well at lengths over 50 m but have a slight excess of energy transmission at close range. Various fatalities and severe casualties from these weapons have been recorded in different places.[9] The most significant limitation of the current, less deadly arsenal is the maximum distance over reliably deploying any tool.

In the literature, casualties received by offenders from far less deadly weapons have been studied, such as chemical projectiles, impact guns, and kinetic energy projectiles.[10] While nonlethal guns are intended to minimize the risk of death or severe injury, several reported fatalities and an unknown number of injuries have occurred. Public understanding of these devices also affects the willingness of an entity to utilize them. One analysis of university students' views of less deadly guns used in a situation where a perpetrator deliberately tries to kill officers found nonlethal projectiles and chemical agents to be more acceptable. In contrast, empty hand attacks and police dog bites were less desirable.

Estimates from a good deal of research indicate that vehicle accidents are responsible for 75% of blunt chest trauma injuries, with blunt chest wall trauma accounting for 25% of all fatalities.[11] Hundreds of studies, including pendulum impact loading, drop tests, human corpses, simulation model crashes with volunteer groups, and anesthetized animals, have occurred in the past few centuries. Examples of injury mechanisms include dense, elastic, and inertial responses. Vehicle occupant impact biomechanics has become synonymous with vehicle crash simulation. Various anthropomorphic test dummies (ATD) and passive and active restraint devices were designed with this knowledge. Among the ATDs utilized for both frontal and lateral impact crash tests are Hybrid III relatives of dummy variables besides frontal impact loading and side-impact dummies besides lateral impact loading. Due to these factors, such as a lack of corpses, animals' incorrect scalability to human models, etc., studies have endeavored to develop a finite element method of the human body to be used as a surrogate in virtual crash tests,[12−14] formed finite element systems of the human body only with significant organs.

PU products are commonly utilized in various applications, such as foams, fibers, adhesives, fabrics, sealants, thermoplastics, malleable wax, and hybrid composites. Foams for structural and nonstructural purposes, protective coatings, and transparent, glossy exterior paints are just a few uses. Chemical-resistant solvents, adhesives, sealants, absorbents, biomedical applications, grouting technologies, automobiles, industrial waste treatment, crashworthiness.[15] PU is used primarily for diverse purposes, including its mechanical characteristics.[16,17]

Polyurethane was first synthesized as a supplement to foam rubber during WWII. Later, the flexibility of this revolutionary substance and its potential to substitute limited resources gave birth to various applications. Today, this category of plastic polymers accounts for 7.7% of the global plastic demand since it is manufactured.[18]

The objective of this study was to improve one's understanding of the viscoelastic character of semiclosed cell flexible polyurethane foams, concentrating on the chemical composition's precise formulation of the polyols and isocyanates. For this purpose, physical−chemical properties, dynamic mechanical analysis (DMA), and dynamic tests of the pneumatic launcher were conducted. Also, the glass-transition temperature, thermal expansion, and loss modulus were explored in various foam materials. In addition, microstructural analysis of the foam to evaluate its dynamic stability properties.
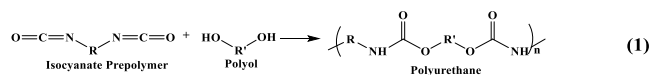
2. EXPERIMENTAL SECTION

2.1. Materials and Chemicals. The polyol used to manufacture polyurethane (90%) content was equal to 60 wt % and was obtained from Confortchem. We also used methylene diphenyl diisocyanate aromatically by 30% NCO, supplied by BASF, which makes up about 30% of all polyurethane supply. The PMDI is used to develop smooth, durable foams for shock absorption. The glycerin GCO (99%) was obtained from Sigma-Aldrich, Germany, and Niax supplied the silicon. A thermoplastic polymer is formed from this reaction. When there are more than dual hydroxyl groups in alcohol, it can create a thermal compound. AcroSeal bestowed the blowing agents, PA, and dichloromethane (98%).

The additives like catalyst triethylenediamine (A-33), obtained from Niax, and PEG (99%) are applied to boost different features of the mixed combination, like cross-link agents, extending-chain agents, puff agents, surfactants, fillers, and plasticizers. The puff agents will form the polyurethane foam, which the surfactants will then reinforce to improve the stability of the polyurethane foam. The fillers for the sand products of VWR PROLAB were 5 and 10 wt % and the graphites were 5 and 10 wt %, acquired from Bental. It has a strong effect on the cohesion of the structure and increases the ability to absorb shocks. In Table 1, we summarize the essential characteristics of our selected fillings.

Table 1. Characteristics of the Used Filler

fillings	density (g/cm^3)	Mohs hardness	specific surface area (m^2/g)	mean size (μm)
sand	2.65	7	0.3–6	2–90
graphite	2–2.25	1–2	6.5–20	6–96

2.2. Characteristics of Polyurethane. Polymerizing polyols form polyurethane by alcohols into two or more reactive hydroxyls connected with the addition of a diisocyanate or polyisocyanate. Chemists have developed a molecule with urethane linkages.[19] Polyurethane foam production is summarized in formula 1

$$\text{O=C=N}{-}R{-}\text{N=C=O} + \text{HO}{-}R'{-}\text{OH} \longrightarrow \left[R{-}\underset{\text{H}}{N}{-}\overset{\text{O}}{C}{-}O{-}R'{-}O{-}\overset{\text{O}}{C}{-}\underset{\text{H}}{N} \right]_n \quad (1)$$

Isocyanate Prepolymer   Polyol   Polyurethane

There seems to be an extensive range of hydroxyl groups and isocyanate compounds, each creating a unique polyurethane content. The characteristics of polyurethane differ depending on its composition. It may have higher strength and rigidity or better elasticity and hardness. The selection of polyol will significantly impact the properties, including the rate of cross-linking in polyurethane products.[20] The number of hydroxyl groups in polyurethane and its molecular size and versatility can be modified significantly to modify the product substance's characteristics. For example, if a diisocyanate reacts with a diol, an elongated, thermoplastic polyurethane is produced. On the other hand, if alcohol contains upwards of two double hydroxyl groups, a stiff thermosetting molecule will result.

2.3. Elaboration of Polyurethane Foams (PU). From a synthesis point of view, the alveolar polyurethane foams are the products of a chemical reaction of a polyisocyanate, polyol, and a blowing agent.[21] This class of polymers can lead to flexible foams, rigid or semirigid, according to the composition and chemical structure of the used reagents.[22] The expected filled polyurethane foam within open cells will be physiochemically characterized and evaluated under dynamic tests.

The elaboration of flexible polymeric foam materials, shockproof in nature, selects the type of polyol, isocyanate, and the most consistent catalyst to arrive at a reliable recipe that allows us to achieve flexible foam with the desired characteristics.[23,24] Obtaining the optimum formulation of PU by free expansion is first carried out in small cups at low stirring speeds (1000 rpm). After each step, all formulations are summarized into four main formulations; the formulation is rectified based on the appearance of the obtained foam. As a result, various formulations are reported in Table 2.

The development of PU in free expansion mode, that is to say, at atmospheric pressure in use is done using a 300 mL volume reactor and mixing using a mechanical stirrer at a speed of 2500 rpm. After thickening of the PU, it is cooled. Then, foam propagation is produced in a preparation vessel. The characteristic times of the production cycle are measured using a digital stopwatch. Finally, the demolding product is left in the open air (for curing) for 24 h before being stored away from light and moisture and then characterized.

The final properties of the polyurethane foam depend on the nature of the chemical components, the blowing agent, the process conditions, and the heart of the mold facings. Thanks to the constant development of new formulations, polyurethane foams are made from various samples today. Therefore, several test pieces were made based on different formulations.[25]

The pneumatic launcher and a rigid wall were evaluated using four test pieces of nonlethal projectiles. The samples of polyurethane foam (PU) made in the laboratory are cylindrical with a convex spherical head glued to a holder made of high-density polyethylene (HDPE) realized by a 3D printer. They were done to highlight the effect of the variation in the machining direction on the mechanical behavior of dynamic tests. Figure 1 depicts a specimen referenced XM1006 nonlethal projectile (Ep_R) and manufactured nonlethal projectiles of various optimal formulations. Different nonlethal projectiles are designed based on existing models in the market.

The XM1006 projectile was produced by the US Army's research laboratories (Exact iMpact) by FW methods and had many features, like a lightweight, a diameter of 40 mm, a length of 10.2 cm, and a muzzle velocity of 85–105 m/s.[26] The head of the projectile consists of foam (4.1 cm in diameter, 6.3 cm in height, 26 g weight, and a 5-year warranty from the date of manufacture). It is stabilized by the included rifling clip and the rifled barrel of the 40 mm launcher. The round is propelled by smokeless powder and has an exceptionally constant velocity.[27] Unfortunately, several deaths have been reported from the XM1006 projectile after hitting the head during riots.[28] As for the pore structure of the XM1006 projectile, the SEM pore structure is unknown because the manufacturer retains the composition and density of the foams that make up the head of the XM1006 commercial projectile. Figure S3 shows the details and dimensions of the nonlethal projectile samples used.

2.4. Physical–Chemical Properties. *2.4.1. X-ray Diffraction Analysis (XRD).* XRD is used to determine the nature of the phases present in porous materials, and structural characterization is mainly carried out by the X-ray diffraction technique (XRD). In polymers, there is no perfect crystal. The partial crystallinity must be considered as the juxtaposition of amorphous zones (where the molecules are disordered) and crystalline zones in which the polymer chains are parallel. There are no long-range molecular arrangements in the amorphous matrix but rather sequences of chain segments that are insufficient to create a crystalline order. As for the crystalline phase, its morphology depends on the crystallization mode of the polymer: mass solidification from the molten state slow crystallization from dilute solutions. From the X-ray diffraction spectra, it is possible to determine the degree of crystallinity.[29] It makes it possible to determine the nature of

Table 2. Essential Compounds in the Preparation of Polyurethane Foams (in wt %)

formulation	polyol	PMDI	catalyst	glycerin	silicon	PEG	dichloromethane	sand	graphite
PU_1	60.24	30.23	1.25	1.74	1.12	0.31	0.11	5	0
PU_2	60.69	25.37	0.53	0.72	1.5	0.96	0.23	10	0
PU_3	60.63	30.64	0.5	0.62	1.42	0.69	0.5	0	5
PU_4	60.44	25.64	0.22	1.23	1.3	0.81	0.36	0	10
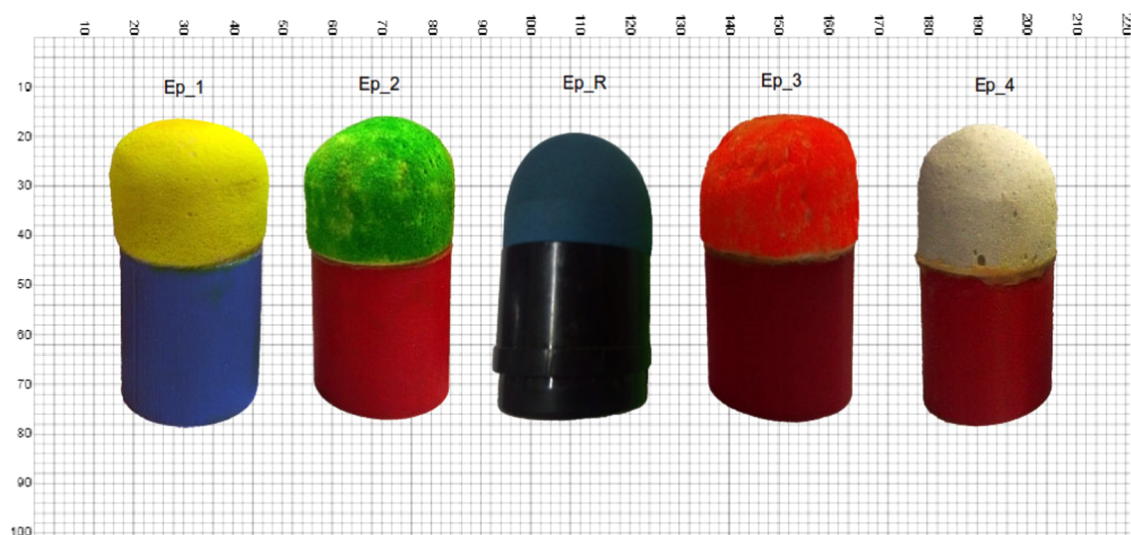
Figure 1. Fabricated and commercial samples of nonlethal projectiles.

the studied body and its structure using the single-crystal methods with a Bragg–Brentano montage, which allows us to choose the inter-reticular distances. These are the most common and easiest methods to implement.

Structural XRD analysis of alveolar PU was carried out on an ITALSTRUCTURES brand diffractometer, model APD 2000, designed for powders and polycrystalline materials. The device is equipped with a GD 2000 goniometer managed by WinDust32 data management and operating software.

The origin 5.0 software using the Gaussian function is used to deconvolution the diffractogram, to determine the ratios of the amorphous and crystalline parts, the peak areas given by the WinAcq32 software are well used. Moreover, the APD 2000 system uses the principle of X-ray reflection by crystalline materials. This phenomenon obeys Bragg's law

$$\lambda = 2d \times \sin \theta \tag{2}$$

where λ is the wavelength of the X radiation used at 1.5418 Å, d is the distance between the planes, and θ is the angle of incidence of the X-rays on the aircraft. The radiation used is of the Cu Kα type with a 40 kV and 30 mA voltage and an angle speed of 0.01°/s.

2.5. Dynamic Characterization. *2.5.1. Dynamic Mechanical Analysis (DMA).* A Mettler Toledo dynamic mechanical analyzer (DMA), SDTA861e, was used to determine the amplitudes of force, displacement, and phase changes. In this case, the tested specimens will be rectangular specimens with 5 mm edges. The samples were heated to a temperature of −80 to 200 °C. The applied force was 0.01 N, with an accuracy of 0.001 N, the frequency of 0.01 Hz, and the imposed deformations could be between 1 and 240 μm, with an accuracy of 0.1 μm, and strain of 0.01% at 1 Hz frequency with 20 steps, with a heating rate of 1 °C/m. The mode of compression oscillation was employed.

2.5.2. Pneumatic Launcher. Four samples were tested, each containing three examples of the same composition as cylindrical test pieces prepared from known formulations. The sample is placed inside the pneumatic launcher, where a constant pneumatic pressure is applied. All of the data related to this test are shown in Table 3.

Several tests were performed on samples made of prepacked polyurethane foam, and nonlethal laboratory projectiles were

Table 3. Characteristics of the Used Nonlethal Projectile

projectile polyurethane foams	length (mm)	diameter (mm)	weight (g)
Ep_1	60	30	25.23
Ep_2	61	31	29.54
Ep_3	62	32	26.17
Ep_4	60	31	28.95
Ep_R	60	30	27.33

designed and manufactured to standards using the commercial XM1006 as a reference (Ep_R) projectile. The Ep_R projectile allows us to compare the dynamic response of the projectile according to the force of the impact on a solid wall equipped with a piezoelectric force sensor. The projectile displacement signal was generated by the velocity sensor on the solid wall to track the speed and force of the projectile. They are also done using internal tracking by oscilloscope software. When two different devices generate the power and displacement signals, they must be synchronized. The relationship is considered to be the maximum impact force. Therefore, more than one experiment is conducted for each sample where the effects have a different effect on the velocities. In all tests, a pressure of 5 bar is applied to compare the strength of the projectile. Various parts of a compressed air ejector are shown in Figures 2 and S4−S6.

Finite element simulations for functional polyurethane foam subjected to influence by a rigid wall could be aimed at fabricating steel parts comprising a force sensor. The joint assembly has a compact structure and an even distribution of the applied force, with a similar density. Still, different mechanical behavior changes energy absorption and acceleration rate for impact application. We summarize the essential characteristics of the pneumatic launcher that we built according to the standards (Tables 4−6).

2.6. Microscopic Characterization. *2.6.1. Scanning Electron Microscope (SEM).* The foams' cellular structure was investigated using an SEM JEOL-JSM 840SM-840 scanning electron microscope at fixed magnifications and a 10 kV voltage. The samples were examined in the direction of free-rising particles. The average diameters of the pores, the thickness of the walls, and the distribution of pore sizes were determined using ImageJ software (Media Cybernetics, Inc.).

Figure 2. Overall sight of the pneumatic launcher.

Table 4. Mechanical Characteristics of the Materials Utilized in the Numerical Simulation Model

material	density (g/cm³)	Poisson's ratio	Young's modulus (GPa)	comments	yield stress (GPa)
steel	7.88	0.31	210	structural steel	180

Table 5. Characteristics of the Nonlethal Projectile by the Pneumatic Launcher Tests

test	density of PU (g/mm³)	impact velocity (ms⁻¹)	deformation speed (s⁻¹)
Ep_1	0.25	1.35	0.21
Ep_2	0.33	2.26	0.23
Ep_3	0.27	3.48	0.25
Ep_4	0.36	4.19	0.27
Ep_R		5.26	0.29

Table 6. Conditions for the Impact Tests with Pneumatic Launcher Tests

property	parameters for testing
nonlethal projectile engineering	cylinder
average weight of the projectile	27.44 g
average diameter of the projectile	30.80 mm
kinetic energy of impact	1000−4500 N
distance from the target	5 m
temperature used in testing	23 °C

3. RESULTS AND DISCUSSION

3.1. Physical−Chemical Properties. *3.1.1. X-ray Diffraction Analysis (XRD).* The result of PU analysis by XRD gave the diffractogram in Figure 3. Given the crystalline nature of sand and graphite fillers, we characterized them by XRD to determine their exact crystalline nature. The search through the software Win Dust 32 and Win Search confirms that it is indeed loaded with a tetragonal crystalline system (with parameters of mesh $a = b = 3.78$ Å and $c = 9.51$ Å) and a
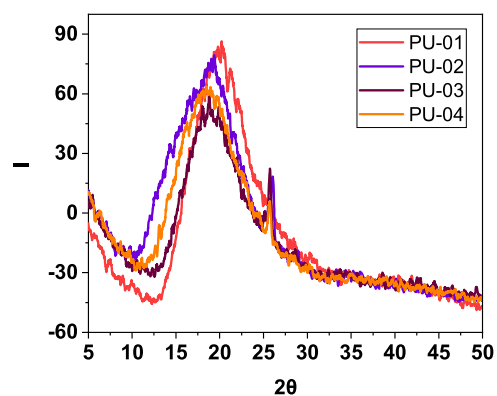

Figure 3. X-ray diffractogram for samples of polyurethane foam.

hexagonal system (with parameters of mesh $a = b = 4.98$ Å and $c = 17.02$ Å).

Taking the sand samples, we can better observe the effect of purification on PEG in the first place by comparing which has been purified locally, and thus a slight increase in the interlamellar distance following the evacuation of impurities such as quartz, pyrite, and plagioclase field paths (calcium albite) in low concentration.

In the XRD diffractogram of PU, we find two prominent peaks of angles 2θ of 19.25 and 25.00°. These indicate a certain degree of crystallinity of our PU, and they are assigned to a dispersion of PU chains with a constant inter-reticular distance (d). The structural morphology of our PU is a semicrystalline type. This semicrystallinity is a partial arrangement of macromolecular chains of PU.

The XRD analysis of the PU with additives and charges gave us the diffractograms in Figures 3 and S1. We deduce that the PU elaborated is of a semicrystalline type, and the addition of additives and charges always leads to a semicrystalline structure. The highest crystallinity is that of the polyurethane foam formulation PU_1, and it decreases after the addition of graphite.

3.2. Dynamic Characterization. *3.2.1. Dynamic Mechanical Analysis (DMA).* The PU foams' dynamic mechanical spectrum (Figure 4) and Figure S7 were recorded versus
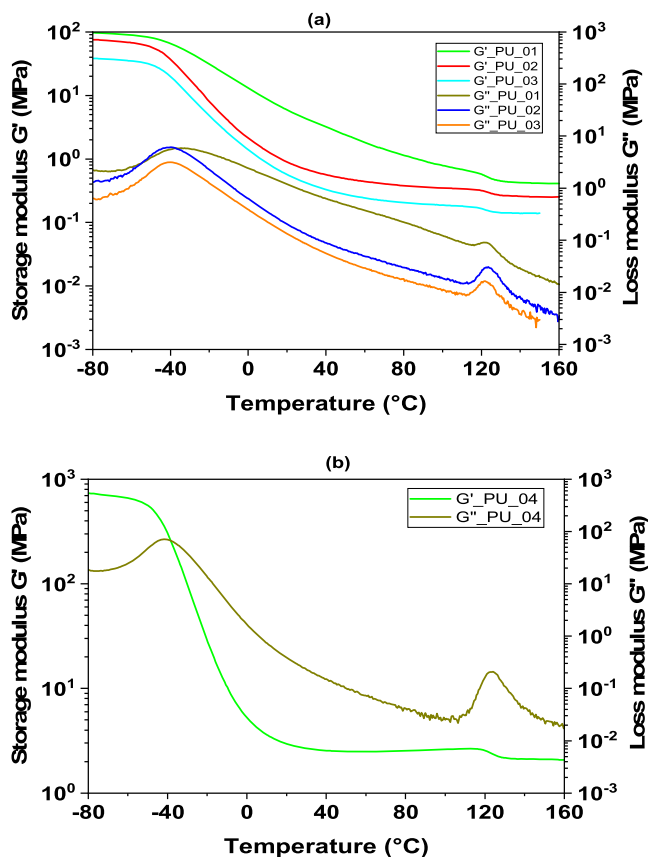

Figure 4. (a) Dynamic mechanical spectra of PU reinforced by sand and (b) analysis results of PU reinforced by graphite; at $T = -80$ at 200 °C, $f = 1$ Hz, and $\Delta T = 3$ °C·min^{-1}.

temperature in the heating mode. Due to the prevalence of macromolecular chains in viscous flow, the polymer material's viscoelasticity improves, and stiffness decreases (Table S1). The modulus values are standardized to three numbers after the comma to describe the absorbing energy properties.[30] The increased number of structural elements controls the movement of polymer chains among themselves, which leads to a rise in the modulus of elasticity.[31] The storage modulus G' increased throughout a wide temperature range when fillers were added to polyols.[32] The results of the dynamic mechanical analysis with a device SDTA861e (DMA) are shown in Figure S2.

In PU_1, PU_2, and PU_3, the storage modulus G' is roughly doubled. G' represents the elastic and reversible energy stored in polymer foams following sand addition. The loss modulus G'' describes the irreversible energy loss of polymer chains' viscoelastic and viscous deformation.[33] At 160 °C, it boosts G'' by adding filler graphite to the PU_4 chain backbone. Higher densities of cross-links and intersegmental connections may increase polymer chain network stiffness.[34] At 122.7, 124.0, and 121.9 °C, the loss modulus of PU foams reaches a maximum. The foaming materials have more viscosity because graphite fillers are added to the chain network;[35] they lower the modulus value for PU_4. The relative height—dampening factor (tan δ max) decreases as the

percentage of G'' to G'. Tan peak intensity fell from 0.16 (PU_1), 0.10 (PU_2), 0.10 (PU_3) and 0.08 (PU_4). Large internal friction distorts the polymer chain network.[36] Large links between the network's soft and hard parts and tight packing make it hard for chain segments to change their shape.[34]

3.2.2. Pneumatic Launcher. The results obtained are summarized in Figure 5. We conclude that the more solid
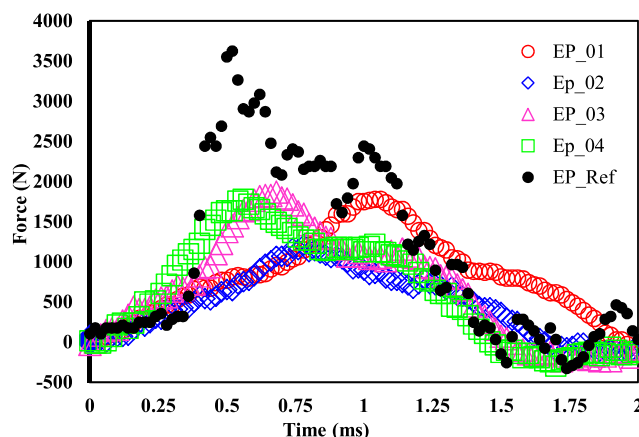
Figure 5. Characteristic force—time of the nonlethal projectile by the pneumatic launcher.

and very dense the sample, the greater the strength and pulse duration. There is a relationship between the microscopic structures of the nonlethal projectile and the actual impact. The results demonstrate a high degree of agreement between the curves of the pneumatic launcher and the reference projectile XM1006 in terms of predicting the maximum head impact force for side impacts. The results of XM1006 are significant for the development of evaluation approaches. There is complete consensus on the nonlethal effects of laboratory-prepared projectiles. Therefore, the maximum force of the impact head can be suggested as the injury criterion.

There is a similarity between experimental test curves for manufactured and commercial projectiles carried out in this work. However, the shock sensor used in the experiments gives good results whenever the impact is significant, which is achieved by the pressure of the air used. The pneumatic launcher tests showed typical behavior of the viscoelastic materials in three phases: linear elastic deformation, plate, and densification. Noting that all samples were applied to their physical properties before and after the test, which stimulated their properties and dimensions, Table S2 summarizes the results.

Tests are carried out on standard-size foam samples to determine their density. However, the stress curve provided by the test results may not be sufficient because the laboratory shock meter is under test and cannot capture the condensation part of the foam pressure. As a result, the curve can be partially extrapolated if necessary. Thus, before any foam material is used confidently in nonlethal projectile impact operations, it must be distinguished by correlated physical tests at the component level. Then, the injury parameters can be predicted with sufficient certainty. Figure S8 summarizes the dynamic impact tests of nonlethal projectiles using a pneumatic launcher. The most important results of the pneumatic
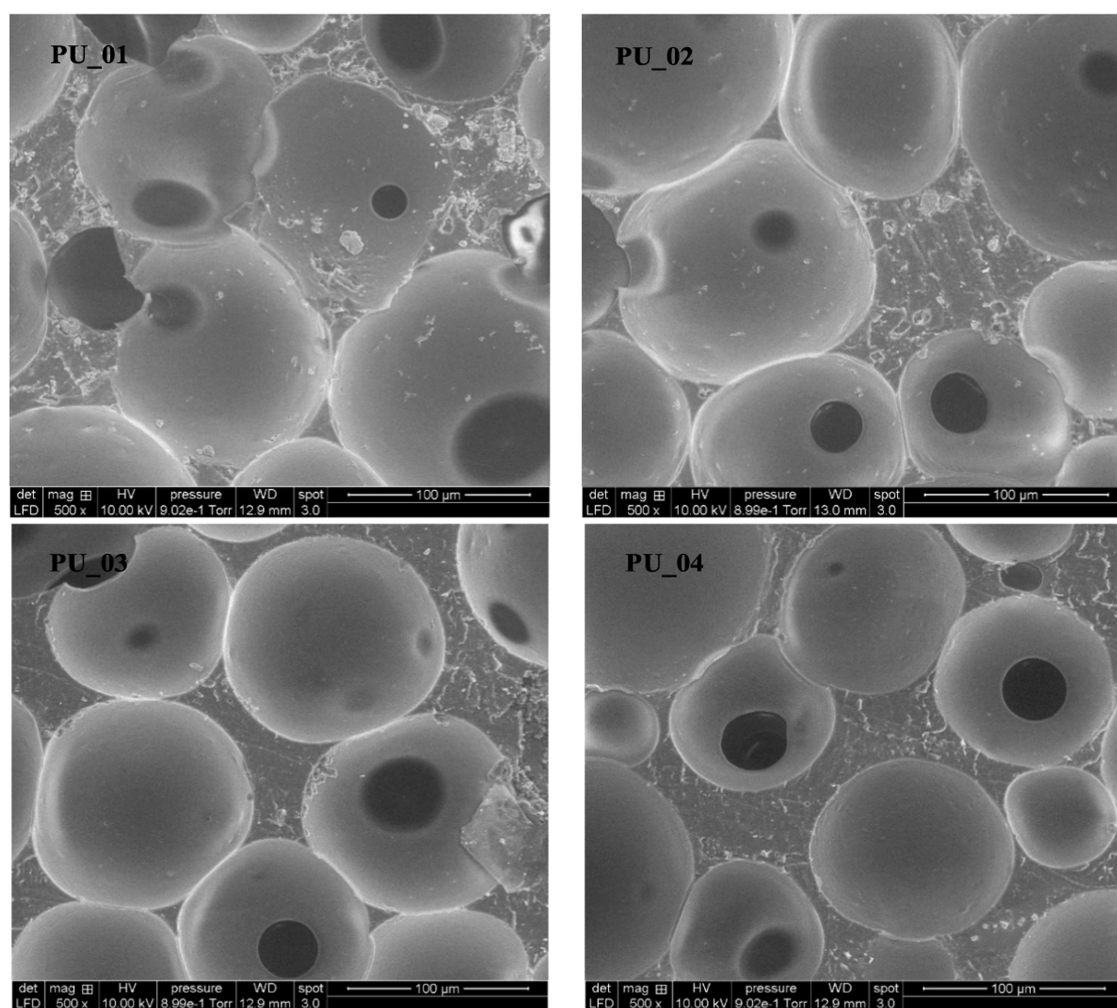
Figure 6. SEM images of the 5 and 10 wt % filled foams.

launcher experiment test for the dynamic characterization of nonlethal projectiles are summarized in Table S2.

Superelasticity and energy absorption are ideally suited for repeated energy absorption or attenuation of vibrations. Sand filler must be fully enclosed inside the architecture of the cells. If the failure of the structures of the cells, the sand filling strength is diminished or lost. Generally, viscoelastic cellular systems should be elastic enough to maintain structural integrity under high dynamic pressure.

The PU cellular microstructure size (about 20 mm) should be decreased. It should be bent to meet the human body shape. Future studies should examine how curved surfaces absorb energy from elastomeric cellular membranes. There should be no loss of superelasticity or reversible energy absorption.

Here, we looked at the dynamic compression of polyurethane cellular structures filled with graphite and sand. As a result, granular materials are excellent shock absorbers. We anticipate that sand-filled cellular formations will perform better under dynamic loads. Dynamic factors (for instance, the micro-inertial effect, the shock wave effect, and the material strain rate effect) also impact nonlethal projectile mechanical behavior.[37] The mechanical characteristics of polymer materials are highly dependent on strain rate. Therefore, future studies will examine the dynamic effects of the cell's sand-filled structure.

3.3. Microscopic Characterization. *3.3.1. Scanning Electron Microscopy (SEM).* The PU foams produced have a consistent cellular structure with an average cell diameter of 98 μm (Figure 6). The amount of sand and graphite included in the polyols did not influence the size and form of the foam cells. For shock absorption, the foam cell wall material's viscoelastic properties are enhanced due to the restricted conformational mobility between entangled chain segments in the cross-linked polymeric chain network and the potential for further hydrogen bonding, limiting the foaming agent's diffusion.

SEM microscopy was used to examine the microstructures of these materials to discover their structure in good agreement with the standard American Standards Testing Methods (ASTM) sheets. These polymers led to single-phase and heterophase materials analyzed from a morphological point of view. Microstructural analysis revealed the open-cell nature of the elaborate foam. The image obtained by the microscope SEM shows open-cell foam partially. Given the results obtained, the elaborate pieces appear to have stubborn regular cellular structures with remarkable overlap reversibility in Figure 6. Cell membranes are visible between the walls of some cells. However, the majority of cells show the absence of membranes. Foam with open or partially open cells is generally soft or semiflexible foam. In our case, the partially open-cell structure is consistent with the soft nature of the foam.

G

We calculated the average pore diameter distribution for different polyurethane products using open-source ImageJ analysis software. Figure S9 presents the obtained results. In addition, the particle size distribution of polyurethane foam cells is summarized in the accompanying Table S3.

Different nucleation processes produce a variety of initial gas cell sizes. Inside these cells, the pressure is greater than the strength of the saturated liquid with gas in which the cells are formed. As it turns out, when a distribution of cell sizes exists, the smaller bubbles are subjected to significantly greater pressures than the more giant cells, which face more significant forces from the big expanding bubble.

As the filled polyurethane foam develops, cells form as gas bubbles develop. The liquid layer becomes thinner within each cell, causing cell window drainage. A critical threshold is achieved when different instabilities set in, leading these cell membranes to break. The breach causes cell coalescence, raising the average size of the cells and widening the cell size dispersion.

Because air bubbles are superior to the polymer solution medium in terms of their dissemination weight, they have a penchant for rising to the foam's surface. This process results in the bubbles rising and creaming fast at the top of an air foaming system with low-viscosity and giant bubbles. Another process closely linked to cream is flocculation, which occurs when particles cluster and stay together. Flocculation is a natural process that increases particle or bubble size, which increases creaming rates.

We manage these instabilities to obtain the appropriate cell shapes and foam properties depending on the method used for foaming with the addition of fillers (sand and graphite). The creaming and flocculation processes will be significant in low-viscosity polyurethane foam systems, depending on the surface-active chemicals included in the system.

While decreasing particle size fills with sand at 5% weight improves PU foam fusion, increasing particle size fills with graphite at 10% weight improves melt strength, resulting in a more uniform distribution of cell size and a decrease in the proportion of open cells. As a result, the mechanical characteristics of the material are enhanced.

3.4. Evaluating the Mold Facings for Projectile Design.

After defining the final product composition of the nonlethal projectile holders, we designed and manufactured these holders based on nanocomposites, high-density polyethylene reinforced. In addition to installing the nonlethal projectile heads consisting of polyurethane foam in the HDPE holders, the corresponding image shows the expected shape of the nonlethal projectile. Finally, we summarize the results in Figure S10.

By analyzing the MEF of the XM1006 reference projectile holder models, we concluded that they are simple to install and consist of a cylindrical inner bore, so we studied the static pressure using the finite element approach. In addition, we created different grids to check projectile holder geometry to determine which grid type would help us achieve the best results. We note that the outcome begins to stabilize across all of the nodes in 200 000. They validate our choice to utilize a tetrahedral network with an algorithm compatible with parametric surfaces and intermediate smoothing. Fast and accurate circumferential drilling with high surface quality 3D in the diagram displays our experimental approach in Figure S11.

Furthermore, we found that the propagation of forces and deformations was linear, so the material generally has solid viscoelastic properties. The exact configuration is the product of the loads applied, and most forces also deform the regions of the holder for the nonlethal projectile. The highest degree of force is located near the top limits of the effect of the collision force on the surface facing the projectile impact. Therefore, when a load is applied to the structure, we notice increased stresses, deformations, and displacements. When comparing PLA with ABS, PLA has better results than ABS for fatigue, displacement, and deformation. Still, we remark that the nonlethal projectile carrier block produced by ABS has a lower mass than PLA, and PLA and ABS properties for making nonlethal projectile holders are in Table S4.

3.4.1. Evaluation of Dynamic Search. We tried as much as possible to get out of the shell of the impact simulations that have been conducted in many pieces of literature as an alternative. It is clear that the human head and chest area are the most sensitive areas to shocks, and most deaths are because of damage to these areas. The force response, skew reactive, and VC_{max} rates were in perfect agreement with those acquired from experimental tests. Likewise, the force response, time response, skew time response, and VC_{max} estimates were in excellent agreement with those received from the paired cadaver tests from the literature. The main drawback in this relationship is the dependence of VC_{max} on the point of impact. Therefore, more influence operations are required to use the average VC_{max} estimates.

Since VC_{max} correlates well with chest hits on the shortened casualty scale, our candidate's experience serves the objective of validating nonlethal weapons produced in our lab (artificial human head). Developed from the optimal formula through 5 years of research and innovation to assess acute ballistic impact trauma, the physical alternative to ballistics and explosives only (our nonlethal projectiles) requires an expensive experimental setup and a cumbersome assessment process. Due to the limitations of use in the civil and military environments, it will be necessary to employ a higher number of effects to gain the appropriate skew response or carry out sampling or average to obtain VC_{max} values. The main drawback with physical alternatives is the necessity of prototyping the products, which is another costly and burdensome thing. Our projectiles do not require an impact simulation since there is no equivocation at the point of impact. They do not need any prototyping because the experiments we used were critical.

3.5. Excessive Force and Casualties.

3.5.1. Viscous Criteria (VC_{max}). Lau and Viano proposed the viscous criteria (VC) in 1986. They conducted many tests wherein races of corpses were exposed to lateral impact stresses simulating automobile collisions. VC based on maximal chest abduction and compression rate (VC_{max}) proved a superior injury predictor. Therefore, VC_{max} is valued and may be represented in terms of the fractal dimension scale.[38−40]

In standards such as ECE-R94, EuroNCAP, ECE-R95 (Impact additionally front), and FMVSS-214, VC_{max} = 1 m/s was defined as the standard for occupant injury risk. Military and defense groups have also evaluated VC_{max} as 1 m/s for nonlethal weapons. The side-impact dummy and the front use the viscosity criteria formula 3.

$$VC = S \times \left(\frac{dY}{dt}\right) \times \left(\frac{Y}{D}\right) \tag{3}$$

where VC is a Viscous Criterion, S is a factor of scale, Y is the chest dip, D is constant, and dY/dt is the rate of chest movement. Values depend on the ATD that is utilized in

vehicle crash testing. Viano and Lau recommended 1.3 m and 181 mm for human cadavers. Using the equation above, we can calculate the maximum chest deformation. Validation of nonlethal projectiles, chest protection, and VC_{max} values is necessary.

We measured the dynamic deflection response of the artificial human head and the time required to achieve the most excellent deflection and maximum deformation velocity. In addition, we recorded VC_{max} values to check nonlethal projectiles using eq 3. Use a scaling factor of 1.3 and a deformation constant of 100 mm.[41] The viscous criteria (VC_{max}) calculation method is presented in Table S5.

The round's type and velocity do not limit the range of injury sustained by kinetic energy weapons and ammunition. It is also about the human tolerance for shock and the viscous criteria (VC_{max}). Females with osteoporosis are more prone to bone fractures than young, healthy males. The heart's ventricular fibrillation caused by the straight impact may be linked to a preexisting condition. Human tolerance cannot be defined by a single number, like projectile speed.

4. CONCLUSIONS

A polyurethane foam reinforced with additives and 5−10% additives and fillers to support foam cell structures to effectively absorb shock and improve the viscoelastic properties of rigid polyurethane foam has been prepared.

The PU diffractogram shows two prominent peaks at angles 2θ of 19.25 and 25.00°. Adding and charging always leads to a semicrystalline structure; hence, the PU developed is semicrystalline. PU_1 has the highest crystallinity and decreases after the addition of graphite.

When fillers were added over in a wide temperature range, the storage modulus G' increased. The storage modulus G' is roughly doubled in PU_1, PU_2, and PU_3. It increases G'' at 160 °C by adding filler graphite to the PU_4 chain backbone. At 122.7, 124.0, and 121.9 °C, the loss modulus of PU foams reaches a maximum. The foaming materials have more viscosity because of graphite fillers added to the chain network. Tan δ max (relative height−dampening factor) decreases as the percentage of G'' to G' increases. Tan peak intensity fell from 0.16 (PU_1), 0.10 (PU_2), 0.10 (PU_3), and 0.08 (PU_4). Large links between the network's soft and hard parts and tight packing make it hard for chain segments to change their shape.

The curves of the pneumatic launcher forecast the highest head impact force for side strikes. All nonlethal projectiles displayed normal viscoelastic material behavior in three phases: linear elastic deformation, plate, and densification. The sand filler must be entirely encased in cell architecture to perform under dynamic pressure. Viscoelastic cellular systems should be able to withstand significant dynamic pressure. We focused on the dynamic compression of polyurethane cellular structures using graphite and sand. As a result, granular materials absorb stress well.

Microstructural analysis revealed the open-cell nature of the elaborate foam. The intricate parts appear to have rigid cellular structures with overlap reversibility. We used ImageJ to calculate the average pore diameter distribution. The liquid layer thins within each cell, generating cell window drainage. Different instabilities cause these cell membranes to rupture at a critical level. The break induces cell coalescence, increasing the average cell size and decreasing size dispersion. While lowering particle size fills by 5% weight of sand enhances PU foam fusion, increasing particle size fills by 10% weight of

graphite increases melt strength, resulting in a more uniform distribution of cell size and a decrease in the number of open cells. As a result, the material's mechanical properties improve.

By evaluating the MEF of the XM1006 reference projectile holder models, we created and built these nonlethal projectile holders. We discovered that forces and deformations propagated linearly, indicating viscoelastic characteristics. The maximum degree of force is near the top of the collision force effect on the nonlethal projectile impact surface.

We tried as much as possible to get out of the shell of the impact simulations that have been conducted in many pieces of literature as an alternative. For acute ballistic impact shock assessment, we fabricated a prosthetic human head. The force response, skew reactive, and VC_{max} rates were in perfect agreement with those acquired from experimental tests where the force response. We measured the artificial human head's dynamic deflection response and how long it took to reach its maximum deflection and deformation speed. The kind and velocity of kinetic energy weaponry and ammunition do not affect the range of harm. It also deals with stress tolerance and the viscous criteria (VC_{max}).

The created nonlethal projectiles outperform commercial ones in impact strength and pressure, supporting the study's efficiency and quality. This study may be used to assess the potential for injury. In addition, they can be applied to make nonlethal kinetic weapons safer.

■ ASSOCIATED CONTENT

ⓈI Supporting Information

The Supporting Information is available free of charge at https://pubs.acs.org/doi/10.1021/acsomega.2c01736.

> X-ray diffractogram for samples of polyurethane foam; mechanical dynamic analysis (DMA) results of polyurethane foam; artificial human head installation; overall sight of the pneumatic launcher and head simulator; design of a dynamic study system for advanced nonlethal projectiles; tan δ curves DMA test results; results of the pneumatic launcher effect test are based on speed; histogram of the distribution of the mean pore diameter of the various produced PU; design of nonlethal projectile mounts with optimum physical and chemical properties; nonlethal projectile carrier construction process, custom industrial model design; test results for dynamic mechanical analysis; most important results of the pneumatic launcher experiment test for the dynamic characterization of nonlethal projectiles; calculation of radii values of polyurethane foam cells and filler material; results of the experimental simulated study of nonlethal projectile holders; and calculation method of the viscous criteria (VC_{max}) (PDF)

■ AUTHOR INFORMATION

Corresponding Author

Noureddine Boumdouha − *Laboratoire Génie des Matériaux, Ecole Militaire Polytechnique, 16214 Algiers, Algeria;* ⓞ orcid.org/0000-0002-8070-490X; Phone: +213-697-005-578; Email: boumdouhanoureddine@gmail.com

Authors

Zitouni Safidine − *Laboratoire de Chimie Macromoléculaire, Ecole Militaire Polytechnique, 16214 Algiers, Algeria*

Achraf Boudiaf − *Laboratoire Génie des Matériaux, Ecole Militaire Polytechnique, 16214 Algiers, Algeria*

Complete contact information is available at:
https://pubs.acs.org/10.1021/acsomega.2c01736

■ REFERENCES

(1) Boumdouha, N.; Safidine, Z.; Boudiaf, A. Experimental Study of Loaded Foams During Free Fall Investigation and Evaluation of Microstructure. *Int. J. Adv. Des. Manuf. Technol.* **2021**, DOI: 10.21203/rs.3.rs-792400/v1.

(2) Mohammad, Z.; Gupta, P. K.; Baqi, A. Experimental and Numerical Investigations on the Behavior of Thin Metallic Plate Targets Subjected to Ballistic Impact. *Int. J. Impact Eng.* **2020**, *146*, No. 103717.

(3) Noureddine, B.; Zitouni, S.; Achraf, B.; Houssém, C.; Jannick, D.-R.; Jean-François, G. Development and Characterization of Tailored Polyurethane Foams for Shock Absorption. *Appl. Sci.* **2022**, *12*, No. 2206.

(4) Cox, T. C.; Buchholz, D. J.; Wolf, D. J. Blunt Force Head Trauma from Police Impact Weapons: Some Skeletal and Neuropsychological Considerations. *J. Crim. Law, Criminol. Police Sci.* **1987**, *15*, 56−62.

(5) Bienert, A. Command Responsibility and the Use of Force by the Police. In *The Police and International Human Rights Law*, Alleweldt, R.; Fickenscher, G., Eds.; Springer International Publishing, 2018; pp 61−82.

(6) Perry, J. M. Joint Doctrine for Nonlethal Weapons. *Army Command and General Staff Coll Fort Leavenworth Ks*, 1999, p 67.

(7) Pollack, E.; Allern, S. Criticism of the Police in the News: Discourses and Frames in the News Media's Coverage of the Norwegian Bureau for the Investigation of Police Affairs. *Nord. Rev.* **2014**, *35*, 33−50.

(8) Mangus, B. E.; Shen, L. Y.; Helmer, S. D.; Maher, J.; Smith, R. S. Taser and Taser Associated Injuries: A Case Series. *Am. Surg.* **2008**, *74*, 862−865.

(9) Hubbs, K.; Klinger, D. *Impact Munitions Data Base of Use and Effects*, National Institute of Justice, 2004; pp 1−25.

(10) Magnolia, D. In *Examination of the Utility of Less-than-Lethal (LTL) Systems in an Exercise Simulated with the Joint Tactical Simulation (JTS) Lawrence Livermore National Laboratory*, Presentation at the Meeting of the National Defense Industrial Association, Lethal Defense III, 1997.

(11) Thota, N.; Epaarachchi, J.; Lau, K. T. Development and Validation of a Thorax Surrogate FE Model for Assessment of Trauma Due to High Speed Blunt Impacts. *J. Biomech. Sci. Eng.* **2014**, *9*, No. JBSE0008.

(12) Kalra, A.; Gupta, V.; Shen, M.; Jin, X.; Chou, C. C.; Yang, K. H. Pedestrian Safety: An Overview of Physical Test Surrogates, Numerical Models and Availability of Cadaveric Data for Model Validation. *Int. J. Vehicle Saf.* **2016**, *9*, 39−71.

(13) Iraeus, J.; Brolin, K.; Pipkorn, B. Generic Finite Element Models of Human Ribs, Developed and Validated for Stiffness and Strain Prediction − To Be Used in Rib Fracture Risk Evaluation for the Human Population in Vehicle Crashes. *J. Mech. Behav. Biomed. Mater.* **2020**, *106*, No. 103742.

(14) Sahoo, D.; Coulongeat, F.; Fuerst, F.; Marini, G. In *Comparison of Head Injury Criteria Based on Real-World Accident Simulations under Visual Performance Solution (VPS)*, IRCOBI Conference, 2020; pp 529−542.

(15) Boumdouha, N.; Safidine, Z.; Boudiaf, A.; Duchet-Rumeau, J.; Gerard, J.-F. Experimental Study of the Dynamic Behaviour of Loaded Polyurethane Foam Free Fall Investigation and Evaluation of Microstructure. *Int. J. Adv. Des. Manuf. Technol.* **2022**, DOI: 10.1007/s00170-022-08963-1.

(16) Miller, M. *Polymers in Cementitious Materials*, iSmithers Rapra Publishing, 2005; pp 23−154.

(17) Ghasemlou, M.; Daver, F.; Ivanova, E. P.; Adhikari, B. Polyurethanes from Seed Oil-Based Polyols: A Review of Synthesis, Mechanical and Thermal Properties. *Ind. Crops Prod.* **2019**, *142*, No. 111841.

(18) Gadhave, R. V.; Srivastava, S.; Mahanwar, P. A.; Gadekar, P. T. Recycling and disposal methods for polyurethane wastes: A review. *Open J. Polym. Chem.* **2019**, *09*, 39−51.

(19) Jang, J. H.; Ha, J. H.; Kim, I.; Baik, J. H.; Hong, S. C. Facile Room-Temperature Preparation of Flexible Polyurethane Foams from Carbon Dioxide Based Poly(ether carbonate) Polyols with a Reduced Generation of Acetaldehyde. *ACS Omega* **2019**, *4*, 7944−7952.

(20) Noureddine, B.; Zitouni, S.; Achraf, B.; Amar, O.; Tria, D. E.; Louar, M. A. In *Manufacture of Polyurethane Foam with a Certain Density*, The International Conference on Recent Advances in Robotics and Automation ICRARE'18, 2018; pp 21−30.

(21) Critchley, R.; Smy, V.; Corni, I.; Wharton, J. A.; Walsh, F. C.; Wood, R. J. K.; Stokes, K. R. Experimental and Computation Assessment of Thermomechanical Effects during Auxetic Foam Fabrication. *Sci. Rep.* **2020**, *10*, No. 18301.

(22) Quintero, M. W.; Escobar, J. A.; Rey, A.; Sarmiento, A.; Rambo, C. R.; de Oliveira, A. P. N.; Hotza, D. Flexible Polyurethane Foams as Templates for Cellular Glass-Ceramics. *J. Mater. Process. Technol.* **2009**, *209*, 5313−5318.

(23) Noureddine, B.; Zitouni, S.; Achraf, B.; Tria, D. E.; Amar, O. In *Élaboration et Caractérisation Mécanique Des Mousses Polyuréthanes Modifiés*, Fourth International Conference on Energy, Materials, Applied Energetics and Pollution ICEMAEP2018, Université Frères Mentouri Constantine 1: Constantine, Algeria, 2018; pp 136−142.

(24) Noureddine, B.; Zitouni, S.; Achraf, B.; Tria, D. E.; Amar, O. Élaboration et Caractérisation Mécanique Des Mousses Polymères: Application Aux Projectiles Non Létaux. In *11th Days of Mechanics JM'11−EMP*, Military Polytechnic School (EMP): Bordj El Bahri, Algeria, 2011; pp 24−33.

(25) Noureddine, B.; Zitouni, S.; Achraf, B.; Tria, D. E.; Amar, O.; Louar, M. A. Mechanical and Microstructural Characterization of

Polyurethane Foams. In *8th Chemistry Days JCh8–EMP*, Military Polytechnic School (EMP): Bordj El Bahri, Algeria, 2019; p 169.

(26) Nsiampa, N. Numerical Assessment of Non-Lethal Projectile Thoracic Impacts. Dissertation, Royal Military Academy, 2016.

(27) Wyant, R. T.; Burns, T.; Allgire, J. *Risk Management of Less Lethal Options: Evaluation, Deployment, Aftermath, and Forensics*, CRC Press, Taylor & Francis Group, 2014; pp 58–128.

(28) Suyama, J.; Panagos, P. D.; Sztajnkrycer, M. D.; FitzGerald, D. J.; Barnes, D. Injury Patterns Related to Use of Less-Lethal Weapons during a Period of Civil Unrest. *J. Emerg. Med.* **2003**, *25*, 219–227.

(29) Patel, A. R. Infrared Absorption Spectroscopy. *J. Med. Chem.* **1965**, *8*, 408.

(30) Mizera, K.; Ryszkowska, J. Polyurethane Elastomers from Polyols Based on Soybean Oil with a Different Molar Ratio. *Polym. Degrad. Stab.* **2016**, *132*, 21–31.

(31) Mizera, K.; Sałasińska, K.; Ryszkowska, J.; Kurańska, M.; Kozera, R. Effect of the Addition of Biobased Polyols on the Thermal Stability and Flame Retardancy of Polyurethane and Poly(Urea)-Urethane Elastomers. *Materials* **2021**, *14*, No. 1805.

(32) Noureddine, B.; Zitouni, S.; Achraf, B. A New Study of Dynamic Mechanical Analysis and the Microstructure of Polyurethane Foams Filled. *Turk. J. Chem.* **2022**, DOI: 10.3906/kim-2108-53, Available online: 23.02.2022 (https://journals.tubitak.gov.tr/chem/accepted.htm).

(33) Hilton, H. H. Elastic and Viscoelastic Poisson's Ratios: The Theoretical Mechanics Perspective. *Mater. Sci. Appl.* **2017**, *08*, 291–332.

(34) Riehle, N.; Athanasopulu, K.; Kutuzova, L.; Götz, T.; Kandelbauer, A.; Tovar, G. E. M.; Lorenz, G. Influence of Hard Segment Content and Diisocyanate Structure on the Transparency and Mechanical Properties of Poly(Dimethylsiloxane)-Based Urea Elastomers for Biomedical Applications. *Polymers* **2021**, *13*, No. 212.

(35) Phan, T. H.; Nguyen, V. T.; Park, W. G. Numerical Study on Dynamics of an Underwater Explosion Bubble Based on Compressible Homogeneous Mixture Model. *Comput. Fluids* **2019**, *191*, No. 104262.

(36) Godovsky, Y. K. Thermomechanics of Molecular Networks and Rubberlike Materials. In *Thermophysical Properties of Polymers*, Yuli, K. G., Ed.; Springer: Berlin, 1992; pp 163–210.

(37) Noureddine, B.; Zitouni, S.; Achraf, B. In *Mechanical and Chemical Characterizations of Filled Polyurethane Foams Used for Non-Lethal Projectiles*, 10th European Symposium on Non-Lethal Weapons EWG-NLW, Royal Military Academy: Brussels, Belgium, 2019; p 68.

(38) Franklyn, M.; Read-Allsopp, C. Injury Scoring Systems and Injury Classification. In *Military Injury Biomechanics*, 2nd ed.; Melanie, F.; Peter, V. S. L., Eds.; CRC Press, 2017; pp 35–70.

(39) Adams, J. H.; Doyle, D.; Grahma, D. I.; Lawrence, A. E.; McLellan, D. R.; Gennarelli, T. A.; Pastuszko, M.; Sakamoto, T. The Contusion Index: A Reappraisal in Human and Experimental Non-Missile Head Injury. *Neuropathol. Appl. Neurobiol.* **1985**, *11*, 299–308.

(40) Benefiel, R. C. Positive Administrative Control: Using Social Exchange to Assess Managerial Impacts on Inmate Misconduct. *Justice Q.* **2019**, *36*, 682–717.

(41) Raymond, D.; Crawford, G.; Van Ee, C.; Bir, C. Development of Biomechanical Response Corridors of the Head to Blunt Ballistic Temporo-Parietal Impact. *J. Biomech. Eng.* **2009**, *131*, No. 094506.